RESEARCH ARTICLE OPEN ACCESS

Effect of Annealing On Thin Film Fabrication of Cadmium Zinc Telluride by Single-R.F. Magnetron Sputtering Unit

Dr. Monisha Chakraborty [A,*] and Sugata Bhattacharyya [B]
[A*] Assistant Professor, School of Bio-Science & Engineering, Jadavpur University, Kolkata-700032, India
[B] Project Fellow, School of Bio-Science & Engineering, Jadavpur University, Kolkata-700032, India
*Corresponding Author

Abstract
In this work, formation of $Cd_{1-x}Zn_xTe$ thin films under various annealing-environments, created by layer by layer deposition of individual CdTe and ZnTe targets from a Single-R.F. Magnetron Sputtering unit is investigated. Structural and optical characterization results show that Vacuum Annealing is the best suitable for the formation of better $Cd_{1-x}Zn_xTe$ XRD peaks of higher intensities in comparison to Argon or Nitrogen-Annealing, for a bi-layered deposited CdTe and ZnTe film on glass substrate. The crystallography of the $Cd_{1-x}Zn_xTe$ films formed appeared to be either Cubic or Rhombohedral type. Also, it has been noticed, that the more inert the annealing-environment is, the lesser is the heat loss by the film-substrate and this results in better fusing of the deposited particles to move more from the poly-crystalline to the mono-crystalline structure. Also higher inert environment causes more Cadmium evaporation and this consequently drives the lattice-constant and the band-gap energy of the formed $Cd_{1-x}Zn_xTe$ thin film to move from the CdTe side to the ZnTe side. The method developed here with proper annealing ambiance for $Cd_{1-x}Zn_xTe$ fabrication can be implemented in laboratories lacking in Co-Sputtering machine.

Keywords $Cd_{1-x}Zn_xTe$, CdTe, ZnTe, Single-R.F. Magnetron Sputtering, Vacuum-Anneal, Argon-Anneal, Nitrogen-Anneal

I. Introduction

Cadmium Zinc Telluride (CZT) is a ternary semiconductor alloy, which has found applications in x-rays and gamma rays detectors, nuclear radiation detectors, substrate for epitaxial-growth of IR-detector material HgCdTe, electro-optical modulators, photo-conductors, light emitting diodes and solar-cells [1-6]. The band-gap of this ternary compound CdZnTe lies between 1.45-2.25 eV [7] and it depends on the variation of Zn content within it. CdZnTe is considered to be an excellent material for X-ray and gamma ray detection [8, 9] because of its low leakage currents and high quantum efficiency. This facilitates its operation as detectors in large volume, even at room-temperature [10]. Applications of CZT have also been studied because of its great possibility in the field of medical imaging. Particularly in the field of single photon emission computed tomography (SPECT), the compound has shown great potential. CZT has also found its application in the sphere of positron emission tomography (PET) [11,12], dedicated emission mammotomography [11,12] and surgical oncology. So the importance of CdZnTe as an excellent bio-medical device grade material is undeniable. Sputtering, as a fabrication technology, can be used for batch-production in medium to large substrate areas. Also fabrication of $Cd_{1-x}Zn_xTe$, with user-defined choice of 'x', can be fabricated from co-sputtering machine using CdTe and ZnTe targets [13] or ZnTe and Cd [14] targets and vice-versa. But in laboratories with low infrastructure and lack of better fabricating-machinery can cause hindrance to such fabrication. In view of lack of Co-Sputtering machine, a secondary line of defense can be implemented to create $Cd_{1-x}Zn_xTe$ by individual deposition of layers of CdTe and ZnTe films, one above the other, respectively. Then by supplementing the sample with proper choice of annealing temperature, annealing-environment and time, the crystals of ZnTe and CdTe can be fused together to form $Cd_{1-x}Zn_xTe$. In this respect, the choice of 'x' in the $Cd_{1-x}Zn_xTe$ thin film can be controlled by controlling the deposited mass and consequently the thickness of CdTe and ZnTe layers individually. In this work our objective is to find the types of formation of $Cd_{1-x}Zn_xTe$ planes (*hkl* values) with respect to change of annealing environment and to note the intensities of those planes with change of by a single R.F. Magnetron Sputtering Unit by using individual CdTe and ZnTe sputtering-targets consecutively. Also a study of the lattice-constants, particle-size and strain and UV-Visible spectrum of those annealed-samples are made, to make a comparative study of the impact of annealing-environment on those above parameters. For our experiment, the proposed choice of 'x' was made to be '0.2'.

II. Experimental Details

1.1 Sample Preparation

Glass-slide, having dimensions of 75mm × 25mm × 1.3 mm, was taken as a substrate for sputter deposition. The slide was initially weighed and then it was cleansed by acetone for 15 minutes by using Ultrasonic Cleaner (Piezo-U-Sonic). The sputtering unit used here is "Planar Magnetron Sputtering Unit (Model: 12"MSPT)", manufactured by Hind High Vacuum Co. (P) Ltd., Bangalore, India. The glass-substrate was subjected to shunt-heating at a chamber pressure of 10^{-3} mBar and was raised to a temperature of 200℃. At a chamber-pressure of over 10^{-4} mBar, sputtering was carried out. The input Argon gas was injected at a line-pressure of 1.26 Kg/cm^2. During Sputtering, the chamber pressure was maintained at a fixed value of 0.035 mBar. The Forward Power and the Reflected Power of the RF Generator was maintained at 410 W and 50 W respectively. Sputtering time for the CdTe and ZnTe deposition was controlled as required to obtain the requisite stoichiometry of $Cd_{1-x}Zn_xTe$. After Sputtering, the substrate was allowed to cool-off and the Diffusion Pump was shut-off at a temperature of 50℃. Air was finally admitted into the chamber when the substrate came down to room-temperature, to prevent any unwanted oxidation of the film. Consecutive deposition of single-layer of CdTe and ZnTe were made, to create a bi-layer film of CdTe and ZnTe respectively. The glass substrate was now cut into 4 equal parts of dimensions 18mm × 25mm × 1.3 mm for further experiment. Three of those four new samples were respectively subjected to (a) Vacuum, (b) Argon and (c) Nitrogen-Annealing. The 4th sample was left un-annealed.

1.1.1 Vacuum-Annealing

Here the sample was annealed for 30 minutes at a temperature of around 200℃ in the same sputter unit at a pressure in between 10^{-4}-10^{-5} mBar. The temperature was manually kept constant at around 200℃ with a ± 2℃ error.

2.1.2 Argon-Annealing

Here the sample was annealed in an Argon ambience in the same sputter unit. Initially a vacuum of 10^{-4} mBar was raised inside the chamber and then Argon was injected inside the chamber at a line pressure of 1.26 Kg/cm^2 as before and the chamber pressure was maintained at a value of 0.035 mBar. The annealing time was 30 minutes, at around 200℃ with a ± 2℃ error.

2.1.3 Nitrogen-Annealing

The process here is exactly similar to that as of in the case of Argon-Annealing, except for here Nitrogen is used as the annealing-environment instead of Argon. Annealing time remained 30 minutes and temperature was kept in and around 200℃ with a ± 2℃ error as before.

III. Theory and Calculations

3.1 Analytical Method for Fabrication of $Cd_{1-x}Zn_xTe$ by layer by layer deposition of CdTe and ZnTe

The total thickness of the bi-layered CdTe and ZnTe thin films were proposed to be 250 nm. The proposed choice of stoichiometry was $Cd_{0.8}Zn_{0.2}Te$, as it is very closely related with the available XRD data of the JCPDS file, where a stoichiometry of '$Cd_{0.78}Zn_{0.22}Te$' is available. The thickness of CdTe and ZnTe layers are found by the method as described in [1, 11, 15, 16] and these values for these layers are found to be 208.168 nm and 40.351nm respectively.

IV. . Results & Discussion

4.1 X-Ray Diffraction (XRD) Results

The XRD spectra of the deposited films were recorded on Rigaku Miniflex (from Japan) powder diffractometer. The incident x-rays were emissions from the Copper-Kα lines, with a wavelength of 1.54025 Å. The scanning angle range i.e. 2θ of the diffractometer was kept between 20° to 70°. The vacuum-annealed sample, for e.g., revealed 3 $Cd_{1-x}Zn_xTe$ peaks in XRD, namely planes with *hkl* values of 111, 311 and 400 of cubic-crystallography or 003, 401 and 404 planes of rhombohedral-crystallography, corresponding to standard XRD data of CZT sample from JCPDS file. The '111' $Cd_{1-x}Zn_xTe$ plane of cubic-crystallography lies between the 111 planes of Cubic-CdTe and Cubic-ZnTe respectively, with corresponding JCPDS file number of 150770 or 752086 and 150746 or 800022 respectively. Also the 2θ angle of the probable cubic-$Cd_{1-x}Zn_xTe$ '111' plane, relates with the standard '$Cd_{0.78}Zn_{0.22}Te$' XRD-data in the JCPDS literature of file number 471296, where a similar '003' plane of rhombohedral-crystallography is also found near the same 2θ region. In this regard it should be said, that our obtained CZT peaks can either be of Cubic or of Rhombohedral crystallography, with either of the particular corresponding cubic or rhombohedral planes. A similar identification method of $Cd_{1-x}Zn_xTe$ peaks are carried out for all the other observed CdZnTe peaks in all the other annealed and un-annealed sample i.e. the existence of the observed cubic- $Cd_{1-x}Zn_xTe$ peak between the standard JCPDS cubic-CdTe and ZnTe peaks and also the existence of the observed $Cd_{1-x}Zn_xTe$ peak in the same 2θ region of the standard $Cd_{1-x}Zn_xTe$ JCPDS literature. The

XRD spectra of Vacuum-Annealed, Argon-Annealed, Nitrogen-Annealed and Un-Annealed Sample is shown in Figure 1, 2, 3 and 4 respectively. Table 1, 4 and 7 gives a detailed discussion of the observed $Cd_{1-x}Zn_xTe$ peaks in the Vacuum, Argon and Nitrogen-Annealed samples respectively. Table 2, 5, 8 and 10 provides the results of all the obtained XRD-peaks of the Vacuum, Argon, Nitrogen and Un-Annealed samples respectively. Table 3, 6 and 9 gives the values of the lattice-constant of the observed $Cd_{1-x}Zn_xTe$ peaks, in case of cubic-crystallography, for the Vacuum, Argon and Nitrogen-Annealed samples respectively.

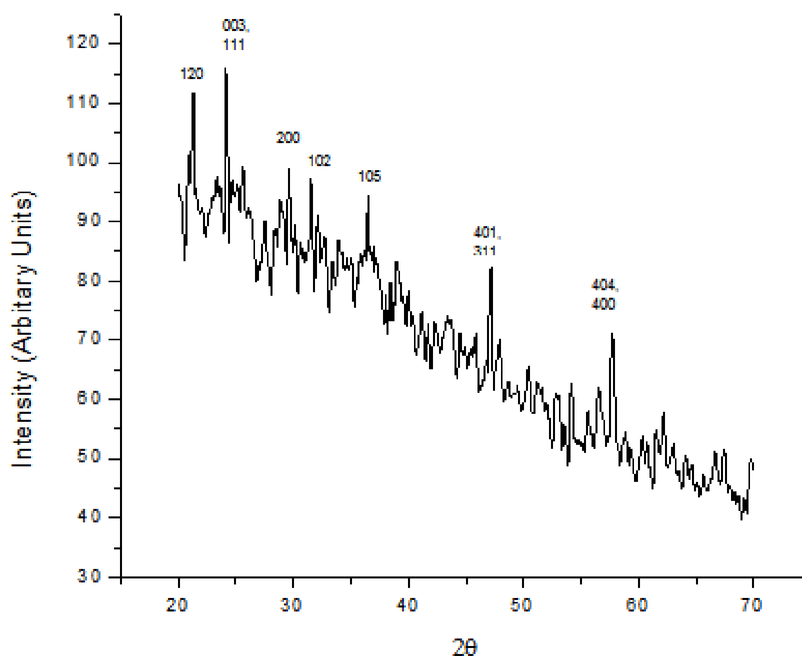

Fig 1: XRD Spectrum of Vacuum-Annealed Sample

4.1.1a. Observed $Cd_{1-x}Zn_xTe$ Peaks of the Vacuum-Annealed Sample

Table 1: $Cd_{1-x}Zn_xTe$ Peaks of the Vacuum-Annealed Sample

Observed $Cd_{1-x}Zn_xTe$ Plane (hkl)	Observed $Cd_{1-x}Zn_xTe$ 2θ (Degree)	Standard Cubic JCPDS CdTe Plane (hkl)	Standard Cubic JCPDS CdTe 2θ (Degree)	JCPDS File No. (CdTe)	Standard Cubic JCPDS ZnTe Plane (hkl)	Standard Cubic JCPDS ZnTe 2θ (Degree)	JCPDS File No. (ZnTe)	Standard JCPDS $Cd_{1-x}Zn_xTe$ Plane (hkl)	Standard JCPDS $Cd_{1-x}Zn_xTe$ 2θ (Degree)	JCPDS File No. $Cd_{1-x}Zn_xTe$
111/003	**24.15**	**111**	**23.757/ 24.027**	**150770/ 752086**	**111**	**25.259/ 25.502**	**150746/ 800022**	**003**	**24.078**	**471296**
311/401	**47.20**	**311**	**46.431/ 46.977**	**150770/ 752086**	**311**	**49.496/ 50.001**	**150746/ 800022**	**401**	**47.111**	**471296**
400/404	**57.75**	**400**	**56.817/ 57.461**	**150770/ 752086**	**400**	**60.632/ 61.289**	**150746/ 800022**	**404**	**57.529**	**471296**

4.1.1b Gross XRD Results of the Vacuum-Annealed Sample

Table 2: Gross XRD Results of Vacuum-Annealed Sample

Observed Angle (Degree)	Compound/Element	Observed Intensity (I/Io)	Observed Plane	Crystal Structure	JCPDS File No.
21.35	CdTe	96.377	120	Orthorhombic	410941
24.15	CdZnTe	100.000	111/003	Cubic/ Rhombohedral	471296 (If Rhombohedral)
29.70	ZnTe	83.611	200	Cubic	800022
31.55	ZnTe	83.772	102	Hexagonal	830966
36.50	Te	81.276	105	Hexagonal	011313
47.20	CdZnTe	70.911	311/401	Cubic/ Rhombohedral	471296 (If Rhombohedral)
57.75	CdZnTe	61.299	400/404	Cubic/ Rhombohedral	471296 (If Rhombohedral)

4.1.1c Lattice Constants of the Observed $Cd_{1-x}Zn_xTe$ Peaks of the Vacuum-Annealed Sample in case of Cubic-Crystallography

The lattice-constant 'a', for cubic-crystallography, of the unit-cell was evaluated by the expression $a = d(h^2 + k^2 + l^2)^{1/2}$, where'd' is the inter-planar distance between the corresponding planes whose Miller index values are (*hkl*).

Table 3: Lattice Constants of $Cd_{1-x}Zn_xTe$ Peaks of the Vacuum-Annealed Sample in case of Cubic-Crystallography

Annealing Type	**CZT Planes (*hkl*)**	**2θ (Degree)**	**d-Value (nm)**	**Lattice Constant 'a' (nm)**	**Lattice Constant 'a' of Standard Rhombohedral $Cd_{1-x}Zn_xTe$ (JCPDS) (nm)**
Vacuum Annealed	**111**	**24.15**	**0.36814**	**0.637**	**0.64**
	311	**47.20**	**0.19236**	**0.637**	
	400	**57.75**	**0.15947**	**0.637**	

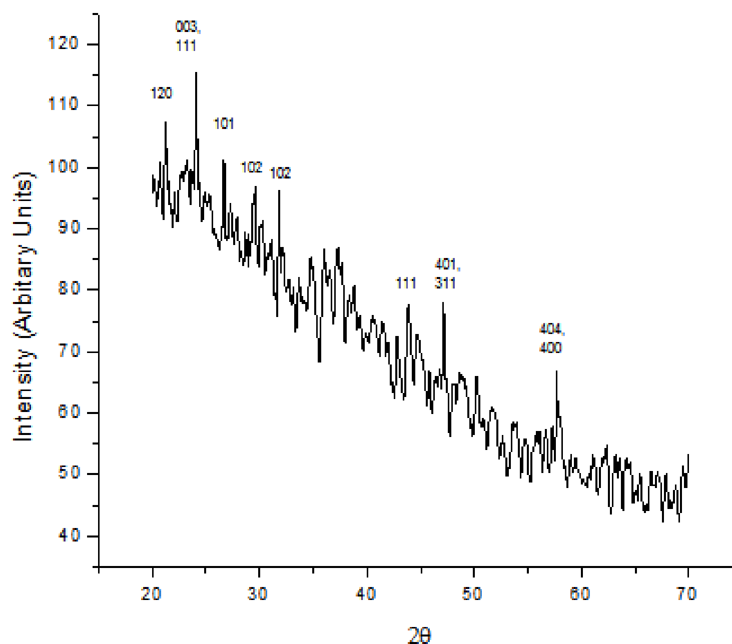

Fig 2: XRD Spectrum of Argon-Annealed Sample

4.1.2a Observed $Cd_{1-x}Zn_xTe$ Peaks of the Argon-Annealed Sample

For the Argon-Annealed sample, a repetition of the same 3 $Cd_{1-x}Zn_xTe$ peaks as in the case of Vacuum-Annealed sample i.e. the planes 111, 311 and 400 or 003, 401 and 404 are found. The peak identification method remains the same as before in the case of Vacuum-Annealed samples.

Table 4: $Cd_{1-x}Zn_xTe$ Peaks of the Argon-Annealed Sample

Observed $Cd_{1-x}Zn_xTe$ Plane (hkl)	Observed $Cd_{1-x}Zn_xTe$ 2θ (Degree)	Standard Cubic JCPDS CdTe Plane (hkl)	Standard Cubic JCPDS CdTe 2θ (Degree)	JCPDS File No. (CdTe)	Standard Cubic JCPDS ZnTe Plane (hkl)	Standard Cubic JCPDS ZnTe 2θ (Degree)	JCPDS File No. (ZnTe)	Standard JCPDS $Cd_{1-x}Zn_xTe$ Plane (hkl)	Standard JCPDS $Cd_{1-x}Zn_xTe$ 2θ (Degree)	JCPDS File No. $Cd_{1-x}Zn_xTe$
111/003	24.10	111	23.757/ 24.027	150770/ 752086	111	25.259/ 25.502	150746/ 800022	003	24.078	471296
311/401	47.15	311	46.431/ 46.977	150770/ 752086	311	49.496/ 50.001	150746/ 800022	401	47.111	471296
400/404	57.70	400	56.817/ 57.461	150770/ 752086	400	60.632/ 61.289	150746/ 800022	404	57.529	471296

4.1.2b Gross XRD Results of the Argon-Annealed Sample

Table 5: Gross XRD Results of Argon-Annealed Sample

Observed Angle (Degree)	Compound/Element	Observed Intensity (I/Io)	Observed Plane	Crystal Structure	JCPDS File No.
21.30	CdTe	93.126	120	Orthorhombic	410941
24.10	CdZnTe	100.000	111/003	Cubic/ Rhombohedral	471296 (If Rhombohedral)
26.65	ZnTe	87.796	101	Hexagonal	830966
29.60	CdTe	83.970	102	Hexagonal	820474
31.80	ZnTe	83.461	102	Hexagonal	830967
43.85	Te	67.437	111	Hexagonal	850555
47.15	CdZnTe	67.541	311/401	Cubic/ Rhombohedral	471296 (Rhombohedral)
57.70	CdZnTe	58.038	400/404	Cubic/ Rhombohedral	471296 (Rhombohedral)

4.1.2c Lattice Constants of the Observed $Cd_{1-x}Zn_xTe$ Peaks of the Argon-Annealed Sample in case of Cubic-Crystallography

Table 6: Lattice Constants of $Cd_{1-x}Zn_xTe$ Peaks of the Argon-Annealed Sample in case of Cubic-Crystallography

Annealing Type	**CZT Planes (*hkl*)**	**2θ (Degree)**	**d-Value (nm)**	**Lattice Constant (nm)**	**Lattice Constant 'a' of Standard Rhombohedral $Cd_{1-x}Zn_xTe$ (JCPDS) (nm)**
Argon Annealed	**111**	**24.10**	**0.36889**	**0.638**	**0.64**
	311	**47.15**	**0.19255**	**0.638**	
	400	**57.70**	**0.15960**	**0.638**	

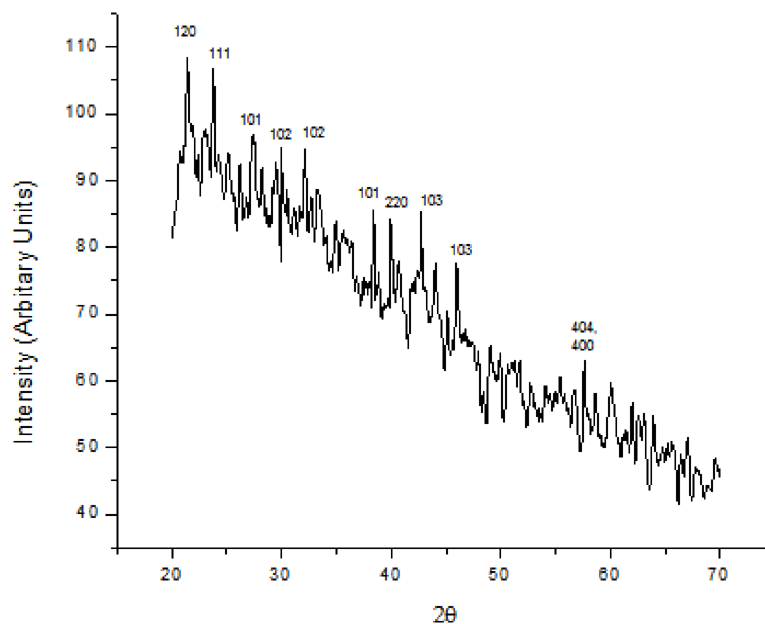

Fig 3: XRD Spectrum of Nitrogen-Annealed Sample

4.1.3a Observed $Cd_{1-x}Zn_xTe$ Peaks of the Nitrogen-Annealed Sample

For the Nitrogen-Annealed sample, the 111 or 003 and the 311 or 401 planes of the $Cd_{1-x}Zn_xTe$ are found to be missing, while the 400 or 404 plane is found to repeat itself. A new plane i.e. *hkl* value of 220 of $Cd_{1-x}Zn_xTe$ has now entered the scene.

Table 7: $Cd_{1-x}Zn_xTe$ Peaks of the Nitrogen-Annealed Sample

Observed $Cd_{1-x}Zn_xTe$ Plane (hkl)	Observed $Cd_{1-x}Zn_xTe$ 2θ (Degree)	Standard Cubic JCPDS CdTe Plane (hkl)	Standard Cubic JCPDS CdTe 2θ (Degree)	JCPDS File No. (CdTe)	Standard Cubic JCPDS ZnTe Plane (hkl)	Standard Cubic JCPDS ZnTe 2θ (Degree)	JCPDS File No. (ZnTe)	Standard JCPDS $Cd_{1-x}Zn_xTe$ Plane (hkl)	Standard JCPDS $Cd_{1-x}Zn_xTe$ 2θ (Degree)	JCPDS File No. $Cd_{1-x}Zn_xTe$
220	**39.95**	**220**	**39.310/ 39.741**	**150770/ 752086**	**220**	**41.803/ 42.252**	**150746/ 800022**	**220**	**39.907**	**471296**
400/404	**57.60**	**400**	**56.817/ 57.461**	**150770/ 752086**	**400**	**60.630/ 61.289**	**150746/ 800022**	**404**	**57.529**	**471296**

4.1.3b Gross XRD Results of Nitrogen-Annealed Sample

Table 8: Gross XRD Results of Nitrogen-Annealed Sample

Observed Angle (Degree)	Compound/Element	Observed Intensity (I/Io)	Observed Plane	Crystal Structure	JCPDS File No.
21.35	CdTe	100.000	120	Orthorhombic	410941
23.75	CdTe	98.474	111	Cubic	150770
27.40	ZnTe	89.298	101	Hexagonal	800009
29.50	CdTe	85.559	102	Hexagonal	820474
32.10	ZnTe	87.379	102	Hexagonal	830967
38.40	Cd	79.065	101	Hexagonal	851328
39.95	CdZnTe	77.564	220	Cubic/ Rhombohedral	471296 (If Rhombohedral)
42.70	CdTe	78.671	103	Hexagonal	190193
46.00	ZnTe	71.635	103	Hexagonal	800009
57.60	CdZnTe	58.031	400/404	Cubic/ Rhombohedral	471296 (If Rhombohedral)

4.1.3c Lattice Constants of the Observed $Cd_{1-x}Zn_xTe$ Peaks of the Nitrogen-Annealed Sample in case of Cubic-Crystallography

Table 9: Lattice Constants of $Cd_{1-x}Zn_xTe$ Peaks of the Nitrogen-Annealed Sample in case of Cubic-Crystallography

Annealing Type	CZT Planes (*hkl*)	2θ (Degree)	d-Value (nm)	Lattice Constant (nm)	Lattice Constant 'a' of Standard Rhombohedral $Cd_{1-x}Zn_xTe$ (JCPDS) (nm)
Nitrogen Annealed	220	39.95	0.22599	0.639	
	400	57.6	0.15985	0.639	0.64

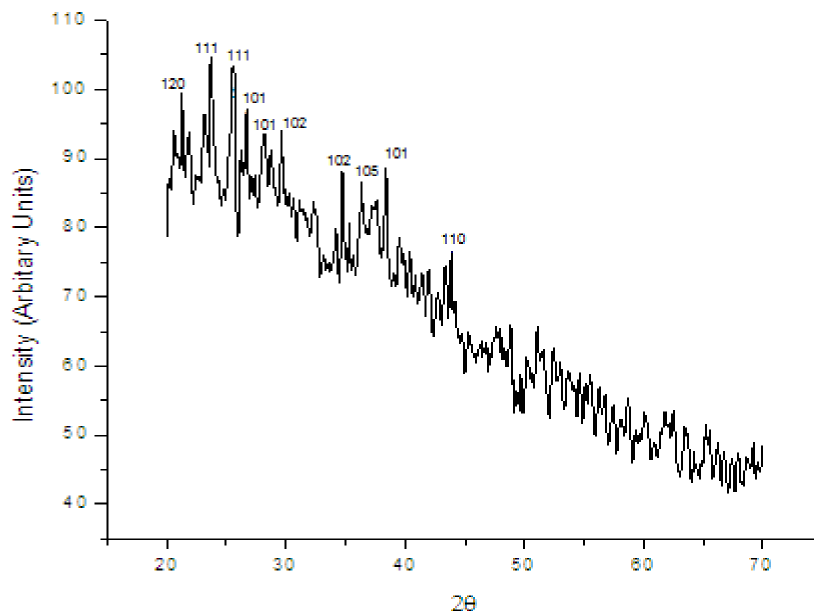

Fig 4: XRD Spectrum of Un-Annealed Sample

4.1.4 Gross XRD Results of the Un-Annealed Sample

The Un-Annealed sample failed to show any CZT peaks, as expected. The presence of various other peaks of CdTe, ZnTe, Cd and Te are found in the XRD result of the sample.

Table 10: Gross XRD Results of Un-Annealed Sample

Observed Angle(Degree)	Compound/Element	Observed Intensity (I/Io)	Observed Plane	Crystal Structure	JCPDS File No.
21.30	CdTe	95.087	120	Orthorhombic	410941
23.70	CdTe	100.000	111	Cubic	150770
25.60	ZnTe	98.915	111	Cubic	800022
26.70	ZnTe	92.816	101	Hexagonal	830966
28.20	Te	89.575	101	Hexagonal	850556
29.60	CdTe	89.855	102	Hexagonal	820474
34.75	ZnTe	84.215	102	Hexagonal	191482
36.40	Te	82.799	105	Hexagonal	011313
38.40	Cd	84.751	101	Hexagonal	851328
43.35	CdTe	71.251	110	Hexagonal	800009

4.1.5 Comparative Study of the XRD Results of all the Annealed and Un-Annealed Samples

A comparative study of the $Cd_{1-x}Zn_xTe$ peaks of the Vacuum, Argon and Nitrogen annealed samples reveal that the CZT planes of *hkl* values of 111, 311 and 400 or 003, 401 and 404 have appeared in both the Vacuum and Argon annealed samples, though there had been a gradual shift of the location of the planes to decreasing 2θ region from Vacuum to the Argon-annealed samples. The Lattice-Constant values of the CZT peaks in the Vacuum and Argon-Annealed samples also show a general increase from the Vacuum to the Argon annealed samples, keeping in tally with their shift of the 2θ values. From Table 3, 6 and 9, the lattice-constants of the possible cubic-planes of the CZT formed under Vacuum, Argon and Nitrogen Annealing is found to be 0.637, 0.638 and 0.639 nm respectively. Also the lattice-constant of the standard rhombohedral $Cd_{0.78}Zn_{0.22}Te$, under the JCPDS file No. 471296, is found to be 0.64 nm. In case of cubic-crystallography, the value of 'x' in $Cd_{1-x}Zn_xTe$ can be obtained as a function of the lattice-constant i.e. 'a' of CdTe, ZnTe and the $Cd_{1-x}Zn_xTe$ formed, by the following equation:-

$$x = \frac{(a_{Cd\,1-xZn\,xTe} - a_{CdTe})}{(a_{ZnTe} - a_{CdTe})} \quad \text{........(1.1)}$$

Where $a_{Cd\,1-xZn\,xTe}$, a_{CdTe} and a_{ZnTe} are the lattice constant of cubic $Cd_{1-x}Zn_xTe$ formed, cubic CdTe and Cubic-ZnTe. Using the lattice constant values of the cubic CdTe from the JCPDS file no. 150770 and the lattice-constant values of the cubic ZnTe from JCPDS file No.150746 and 800022, the value of 'x' in our obtained $Cd_{1-x}Zn_xTe$ peaks of the Vacuum, Argon and Nitrogen-Annealed samples are found out by using Equation 1.1.The results are tabulated in Table 11.

Table 11: Value of 'x' obtained using lattice constants of $Cd_{1-x}Zn_xTe$, CdTe and ZnTe for Vacuum, Argon and Nitrogen Annealed Sample

Annealing Type	Lattice Constant of obtained $Cd_{1-x}Zn_xTe$ (nm)	Lattice Constant of Cubic CdTe (JCPDS File No.150770) (nm)	Lattice Constant of Cubic ZnTe (JCPDS File No.150746) (nm)	Value of 'x'	Lattice Constant of Cubic CdTe (JCPDS File No.150770) (nm)	Lattice Constant of Cubic ZnTe (JCPDS File No.800022) (nm)	Value of 'x'
Vacuum	0.637	0.6481	0.61026	0.2933	0.6481	0.6045	0.2545
Argon	0.638	0.6481	0.61026	0.2669	0.6481	0.6045	0.2316
Nitrogen	0.639	0.6481	0.61026	0.2404	0.6481	0.6045	0.2087

In our experiment, the value of 'x' is 0.2. In our sample of $Cd_{1-x}Zn_xTe$, the value of 'x' cannot be less than 0.2. This is because it will indicate evaporation of "Zinc" before "Cadmium", while the former has a higher melting and boiling point than the latter. So for finding 'x' using Equation 1.11, any combination that uses the value of lattice-constant of cubic CdTe of JCPDS file No. 752086 is rejected, as it will give a lesser value of 'x' than the initial value i.e. 0.2. So, now, by observing the values of 'x' in Table 11, it is clear that value of 'x' increases from the Nitrogen to the Vacuum-Annealed sample. As the Lattice constant of $Cd_{1-x}Zn_xTe$ is function of the value of 'x', the vacuum annealed samples seems to have an increased value of Zinc content, that is higher value of 'x', compared to the Argon annealed ones. This must be because of the fact that increased evaporation of Cadmium took place in the Vacuum-Annealed samples. This increased evaporation of Cadmium can actually be the effect of the vacuum in our experiment ($<10^{-4}$ mBar); which has almost zero convection and conduction. As a result, the heat transfer from the annealed-substrate to the corresponding vacuum ambience is so slow and small, that the deposited films get sufficient heat and time to fuse together with each other and also lead to evaporation of Cadmium from the substrate. Nitrogen annealed sample revealed two CZT peaks of *hkl* planes of 220 and 400 or 404. But the most dominant 111 plane of CZT failed to show up in the Nitrogen annealed sample. Also the lattice-constant of the Nitrogen-annealed CZT planes indicated a higher value corresponding to the Argon and Nitrogen annealed samples. Such higher value of lattice constant indicates less or almost zero Cadmium evaporation from the Nitrogen-annealed-sample. It can be explained on the fact that the Nitrogen being less inert than Argon, has got higher thermal conductivity of 0.024 W/(m.°C) compared to that of Argon of 0.016 W/(m.°C). So higher conductivity of Nitrogen caused quicker heat dissipation from the annealed-substrate compared to that of Argon and provided less heat and time for the deposited layers of CdTe and ZnTe to fuse together and form better CZT planes, though both Argon and Nitrogen-annealed samples were both heated for 30 minutes. Higher value of lattice-constant of Nitrogen-annealed samples, indicating higher presence of Cd, also relates to the same fact of quicker heat dissipation

from the Nitrogen-Annealed samples and less evaporation of Cd. Table 12 gives a comparative summarized analysis of the number of CZT peaks formed and their intensities, under various annealing conditions.

Table 12: CZT Peaks and their Intensities under various Annealing-Conditions

Annealing Type	CZT Plane (111)	Intensity (I/Io)	CZT Plane (311)	Intensity (I/Io)	CZT Plane (400)	Intensity (I/Io)	CZT Plane (220)	Intensity (I/Io)
Vacuum	Present	100	Present	70.91	Present	61.29	Absent	Absent
Argon	Present	100	Present	67.54	Present	58.03	Absent	Absent
Nitrogen	Absent	Absent	Absent	Absent	Present	58.03	Present	77.56
Un-Annealed	Absent	Absent	Absent	Absent	Absent	Absent	Absent	Absent

The above table reflects that the formation of CZT has been most facilitated by the Vacuum-Annealing environment, as is understood by comparing the relative intensities and the number of CZT peaks under Vacuum, Argon, Nitrogen and Un-Annealed conditions. In this respect it might be re-emphasized here that most probably the extreme inert nature of the Vacuum ambience, with almost zero heat conduction and convection, gave better time and more heat for better fusing and formation of CZT peaks. The impact of better inertness of the annealing environment thus seem to have a positive effect on better formation of CZT and the pattern also continues from the Argon to Nitrogen annealing-types. Regarding the exact crystallography of the obtained $Cd_{1-x}Zn_xTe$ peaks, it is possible either the cubic or the rhombohedral type is formed. As the values of 'x' and lattice-constant for e.g. for the Nitrogen-Annealed sample for cubic-crystallography is 0.2404 and 0.2087 (from Table 11) and 0.639 nm respectively, and this lies very close to the standard value of "0.22" of "x" and "0.64 nm" value of lattice-constant, in the rhombohedral type $Cd_{0.78}Zn_{0.22}Te$ in JCPDS file No. 471296, the exact crystallography of the formed $Cd_{1-x}Zn_xTe$ peaks could not be said with certainty in our samples. In this regard it should also be mentioned, that the standard rhombohedral CZT was formed by Travelling Heater-Method and had the angles $\alpha = \beta = \gamma = 89.94°$. So the standard JCPDS Rhombohedral crystallography of CZT has a very thin line of demarcation with possible cubic-crystallography. So, the $Cd_{1-x}Zn_xTe$ peaks in our samples can be either of cubic or of rhombohedral crystallography.

4.2 *UV-Visible Results of all the Samples*

All the 4 samples were subjected to UV-Visible optical test using PerkinElmer Lambda 25 spectrophotometer, with a wavelength ranging from 300-900 nm and the absorption spectra and correspondingly the transmission spectra were obtained from them.

From the optical-data, the molar absorption co-efficient i.e. 'α' is determined by the expression:-

$$\alpha = \frac{1}{d}\ln\left({}^{1}/_{T}\right) \quad \ldots\ldots(1.2)$$

Where'd' is the net thickness of the deposited film and 'T' is the observed transmittance.

The following graphs were obtained, with Band-Gap-Energy (hυ), in eV, as the x-axis and the $(\text{Band-Gap-Energy/nm})^2$ i.e. $(\alpha h\upsilon)^2$ as the y-axis from the UV-Visible data. From such graphs, the band-gap energy of the fabricated thin-films can be calculated [17, 18]. Figure 5, 6, 7 and 8 provides the UV-Visible Result of Vacuum, Argon, Nitrogen and Un-Annealed sample respectively. Table 13 provides the approximate Band-Gap obtained from all the samples.

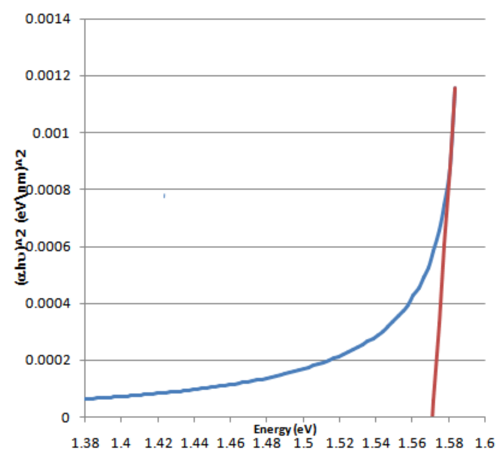

Fig 5: UV-Visible Result of Vacuum-Annealed Sample

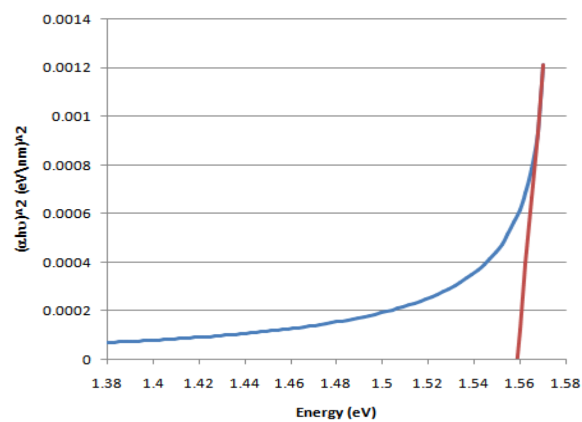

Fig 6: UV-Visible Result of Argon-Annealed Sample

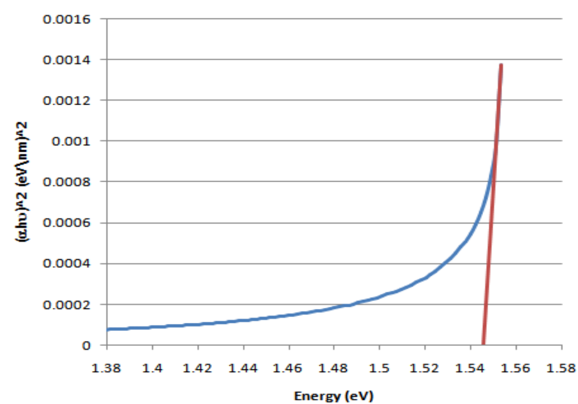

Fig 7: UV-Visible Result of Nitrogen-Annealed Sample

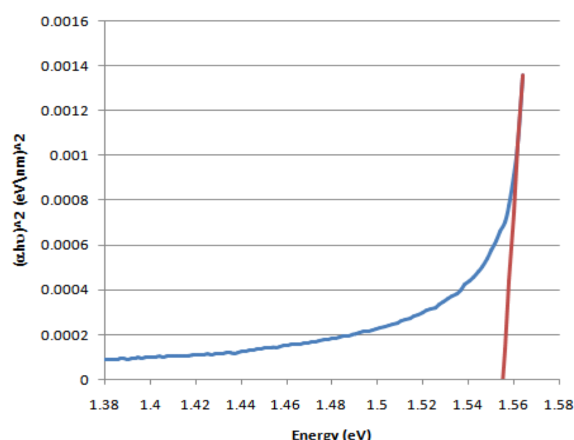

Fig 8: UV-Visible Result of Un-Annealed Sample

Table 13: Approximate Band-Gap of all Annealed and Un-Annealed Sample

Annealing Type	Approximate Band-Gap (eV)
Vacuum	**1.570**
Argon	**1.560**
Nitrogen	**1.545**
Un-Annealed	**1.555**

4.2.1 Analysis of all the UV-Visible Results

The UV-Visible results of the Vacuum-Annealed, Argon-Annealed and Nitrogen-annealed samples are in tally with their corresponding value of lattice-constants of the CdZnTe planes. As there is a general increase in value of the lattice-constants of the CZT planes of the samples from Vacuum-Annealed to Argon-Annealed to Nitrogen-Annealed samples, there is an increasing Cadmium content from the Vacuum to the Nitrogen-Annealed samples. So consequently the band-gap of the samples, from Vacuum to Nitrogen-annealed ones, has shifted more towards the direction of the band-gap of CdTe (i.e. 1.45 eV) from the direction of band-gap of ZnTe (i.e. 2.25 eV), in the corresponding UV-Visible spectrum.

The band-gap value of the Un-Annealed sample is interesting to note, as its band-gap value is almost similar to that of the Annealed-Samples. This may be because of the fact, that the proportion of Cadmium-Telluride is much higher than that of the Zinc-Telluride in our sample, and the UV-Visible result of the Un-Annealed sample is mostly dominated by the band-gap value of CdTe.

4.3 Strain and Particle Size Results of all the Samples

The particle size (L) and strain (ε) for polycrystalline structures can be expressed in a linear combination as a function of FWHM (β) of the XRD peaks and is given by the following equation [9,19]:

$$\frac{\beta\cos\theta}{\lambda} = \frac{1}{L} + \frac{\varepsilon\sin\theta}{\lambda} \quad \text{.......(1.3)}$$

From the $(\frac{\sin\theta}{\lambda}, \frac{\beta\cos\theta}{\lambda})$ graph, the particle size & strain are obtained from the intercept and slope of the above plot in Equation 1.3. Figure 9, 10, 11 and 12 provides the $(\frac{\sin\theta}{\lambda}, \frac{\beta\cos\theta}{\lambda})$ graph of the Vacuum, Argon, Nitrogen and Un-Annealed sample.

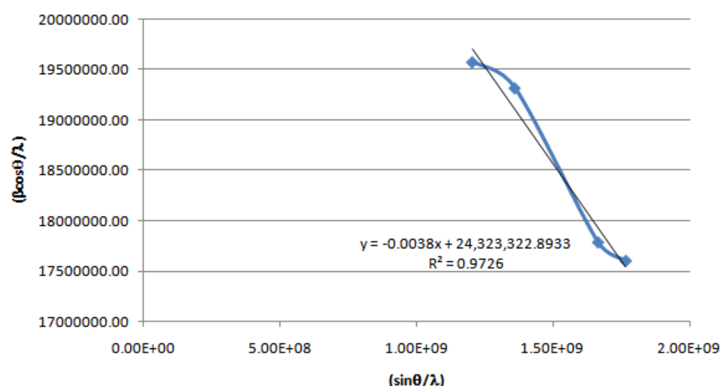

Fig. 9: Variation of $\frac{\sin\theta}{\lambda}$ vs. $\frac{\beta\cos\theta}{\lambda}$ of Vacuum-Annealed Sample

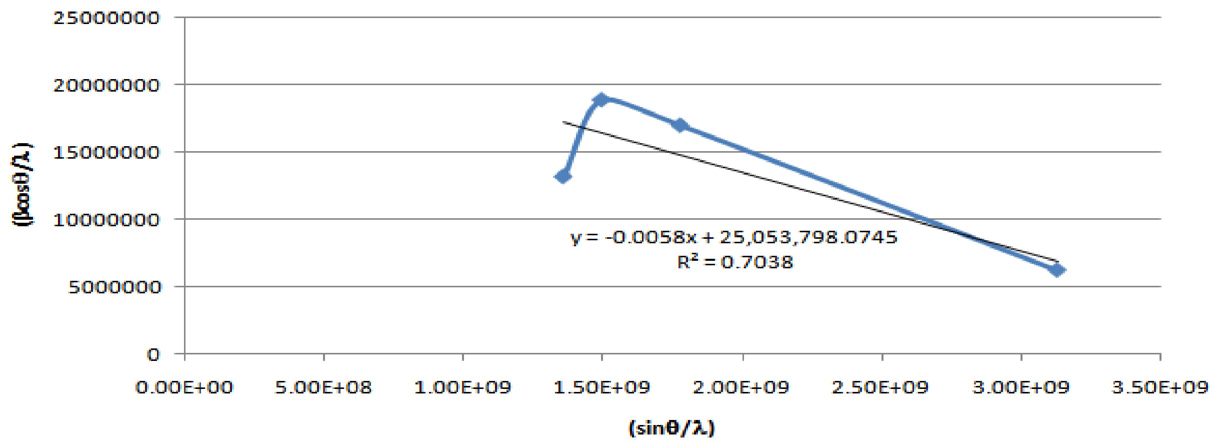

Fig. 10: Variation of $\frac{\sin\theta}{\lambda}$ vs. $\frac{\beta\cos\theta}{\lambda}$ of Argon-Annealed Sample

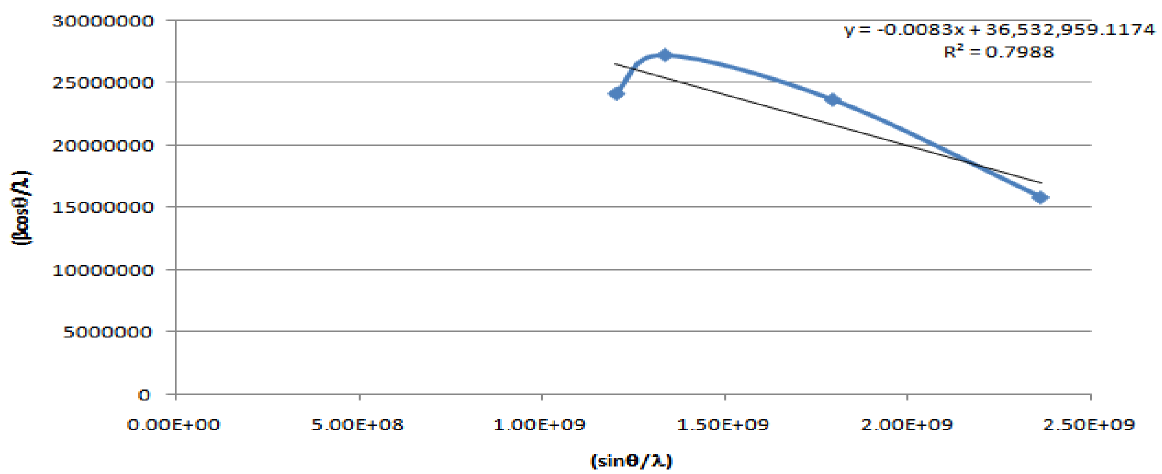

Fig. 11: Variation of $\frac{\sin\theta}{\lambda}$ vs. $\frac{\beta\cos\theta}{\lambda}$ of Nitrogen-Annealed Sample

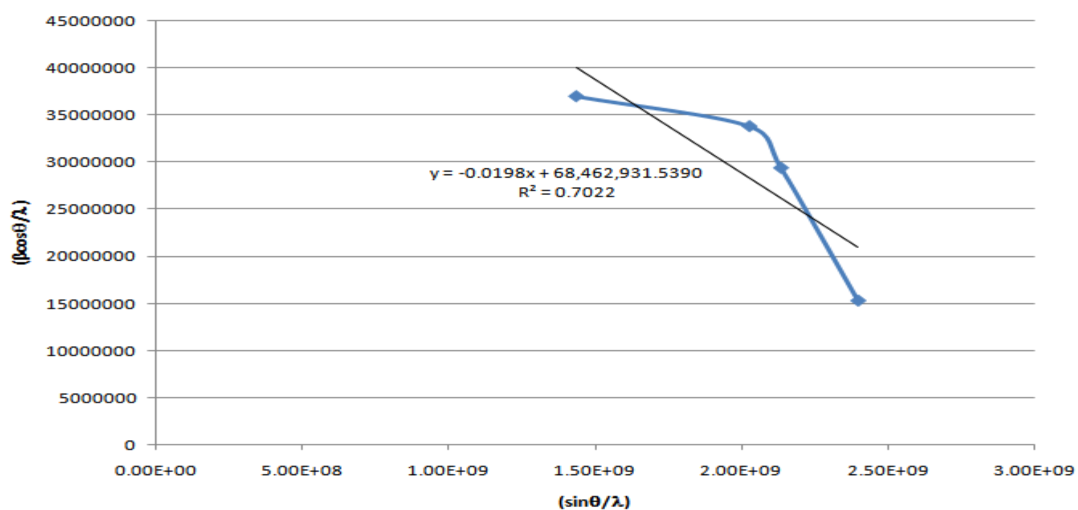

Fig. 12: Variation of $\frac{\sin\theta}{\lambda}$ vs. $\frac{\beta\cos\theta}{\lambda}$ of Un-Annealed Sample

4.3.1 A comparative study of the obtained Particle size and Strain under various Annealing and Un-annealed conditions

Table 14: Particle Size and Strain Value under various Annealing and Un-Annealed Conditions

Annealing Type	Particle Size (nm)	Strain
Vacuum	41.11	-0.0038
Argon	39.91	-0.0058
Nitrogen	27.37	-0.0083
Un-annealed	14.60	-0.0198

Table 14 provides the various particle size and strain value under various annealing and un-annealed condition. It is observed that there is an increasing value of particle-size along with a decreasing value of compressive-strain (indicated by negative sign) from the Un-annealed to the Vacuum-Annealed sample. It can be proposed here and can be tallied with XRD peaks and their corresponding intensities, that under Vacuum-Annealed condition the CdTe and ZnTe particles received comparatively higher heat (and lesser heat loss) to produce more fused and larger particle size. Also the decreasing value of compressive-strain suggests that under Vacuum-Annealing condition, the crystalline structure changed maximum from polycrystalline to mono-crystalline form and is also strengthened by the fact of increasing particle-size trend. The following strain vs. particle-size curve indicates the above discussion.

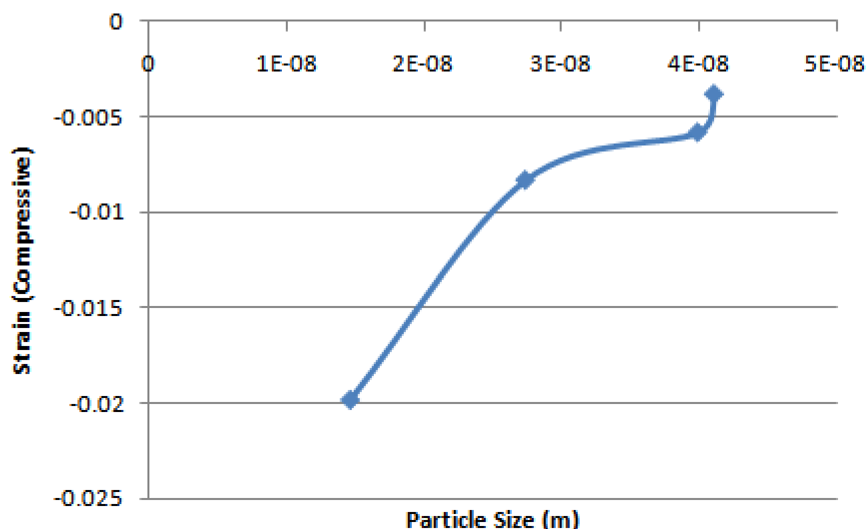

Fig. 13: Variation of Strain vs. Particle Size

V. Conclusion

(1) Vacuum-Annealing is the most suitable environment for better production of $Cd_{1-x}Zn_xTe$ from the layer by layer deposited CdTe and ZnTe films on glass-substrate, forming a bi-layer, from a single R.F. Magnetron Sputtering Unit. The crystals of $Cd_{1-x}Zn_xTe$ are either of Cubic or of Rhombohedral-crystallography.

(2) The more inert the annealing environment is, the less the heat is lost by the substrate and the film and more the heat it gets to form CZT. Also, higher inert environment tends to cause more Cadmium evaporation from the substrate and consequently shifts the lattice-constant and the band-gap energy towards the direction of ZnTe, from the CdTe side.

(3) Bigger particle size is obtained in case of a better inert environment, thus implying the change of the crystal structure from the poly-crystalline to the mono-crystalline form.

VI. Acknowledgement

Authors are very much thankful to University Grants Commission, Government of India, for providing financial support for this work.

References

[1] M. Chakaborty, Fabrication of Nano-structured Cadmium Zinc Telluride thin films, International Journal of Engineering Research and Applications (IJERA), Vol. 2, Issue 1(2012) 1126-1134

[2] D. Zeng, W. Jie, T. Wang, W. Li, J. Zhang, The relationship between stress and photoluminescence of $Cd_{0.96}Zn_{0.04}Te$ single crystal, Materials Science and Engineering B 142 (2007) 144–147.

[3] J. P. Faurie, J. Reno, M. Boukerche, J. Crystal Growth, 72 (1985), 111.

[4] T. E. Schlesinger, R. B. James, Semiconductors and Semimetals, edited 43, Academic, San Diego (1995).
[5] R. Dornhaus, G. Nimitz, G Höhler, E. A. Nickisch, Springer (1983), 119.
[6] Z. Q. Shi, C. M. Stahle, P. Shu, Proc. SPIE. 90 (1998) 3553.
[7] K. Prabakar , S. Venkatachalam , Y. L. Jeyachandran , Sa.K. Narayandass , D. Mangalaraj, Microstructure, Raman and optical studies on Cd0.6Zn0.4Te thin films, Materials Science and Engineering B107 (2004) 99–105.
[8] J. Gaines, R. Drenten, K. Haberbern, P. Menz, J. Petruzzelo, Appl. Phys. Lett. 62 (1993) 2462.
[9] J. Pal, PhD Thesis, Jadavpur University, Kolkata, India, 2005.
[10] Q. Li , W. Jie, Li Fu, X. Zhang, X. Wang, X. Bai, G. Zha, Investigation on the electrical properties of metal–$Cd_{0.9}Zn_{0.1}Te$ contacts, Materials Science and Engineering B 135 (2006) 15–19.
[11] M. Chakaborty, A Study Of Dimensional Effect On Structural Properties Of Cadmium Zinc Telluride Thin Films, International Journal of Engineering Research and Applications (IJERA), Vol. 1, Issue 4, 2096-2104
[12] M. Chakaborty, Estimation Of 'X' In $Cd_{1-X} Zn_xTe$ Thin Films Using X-Ray Diffraction Analysis, International Journal of Engineering Research and Applications (IJERA), Vol. 2, Issue 2 (2012) 994-1001
[13] http://etd.fcla.edu/SF/SFE0000341/ThesisCZT.pdf ,J. Gadupati, Master of Science Thesis, University of South Florida, Florida, USA, 2004.
[14] M. Becerril, H. Silva-Lope, O. Zelaya-Angel, Band gap energy in Zn-rich $Zn_{1-x}Cd_xTe$ thin films grown by r.f. sputtering, Revista Mexicana De Fisica 50 (6) (2004) 588–593.
[15] M. Chakraborty, Optimum Stoichiometry Of Cadmium Zinc Telluride Thin Films In The Light Of Optical,Structural And Photon Generated Gain Studies, International Journal of Engineering Science and Technology (IJEST), Vol.3, No. 5 (2011) 3800.
[16] M. Chakraborty, Dimensional Effect on Optical Properties Of Cadmium Zinc Telluride Thin Films, International Journal of Engineering Science and Technology (IJEST), Vol.3, No. 10 (2011) 7402-7407
[17] G. P Joshi, N. S. Saxena, R. Mangal, A. Mishra, T. P. Sharma, Bull. Mater. Sci. 26 (2003) 387.
[18] T. E. Schlesinger, J. E. Toney, H. Yoon, E. Y. Lee, B. A. Brunett, L. Franks, R. B.James, Material Science and Engineering 32 (2001) 103.
[19] S. B. Quadri, E. F. Skelton, D. Hsu, A. D. Dinsmore, J. Yang, H. F. Gray, B. R. Ratna, Phys. Rev. B 60 (1999) 9191.